Nat. Hazards Earth Syst. Sci. Discuss., 3, 5357–5381, 2015
www.nat-hazards-earth-syst-sci-discuss.net/3/5357/2015/
doi:10.5194/nhessd-3-5357-2015

Natural Hazards and Earth System Sciences
Open Access
Discussions

The European lightning location system EUCLID – Part 2: Observations

D. R. Poelman[1], W. Schulz[2], G. Diendorfer[2], and M. Bernardi[3]

[1]Royal Meteorological Institute of Belgium, Brussels, Belgium
[2]OVE-ALDIS, Vienna, Austria
[3]CESI – Centro Elettrotecnico Sperimentale Italiano spa, Milan, Italy

Received: 27 July 2015 – Accepted: 26 August 2015 – Published: 4 September 2015

Correspondence to: D. R. Poelman (dieter.poelman@meteo.be)

Published by Copernicus Publications on behalf of the European Geosciences Union.

Abstract

Cloud-to-ground (CG) lightning data from the European Cooperation for Lightning Detection (EUCLID) network over the period 2006–2014 are explored. Mean CG flash densities vary over the European continent, with the highest density of about $6\,km^{-2}\,yr^{-1}$ found at the triple point between Austria, Italy and Slovenia. The majority of lightning activity takes place between May and September, accounting for 85 % of the total observed CG activity. Furthermore, the thunderstorm season reaches its highest activity in July, while the diurnal cycle peaks around 15:00 UTC. A difference between CG flashes over land and sea becomes apparent when looking at the peak current estimates. It is found that flashes with higher peak currents occur in greater numbers over sea than over land.

1 Introduction

Numerous ground-based lightning location systems (LLS) exist to date employing different types of sensors and detection techniques, enabling the user to detect cloud-to-ground (CG) and/or intra- and intercloud electrical activity. As such, it is possible to retrieve not only the geographical and frequency distribution of lightning on a global scale (Jacobson et al., 2006; Keogh et al., 2006; Said et al., 2010, 2011), but detailed information at the level of individual strokes or flashes as well by means of three dimensional reconstruction of the development of the lightning channel as observed by present-day Lightning Mapping Arrays (LMAs) (Krehbiel et al., 1999; Rison et al., 1999, 2000; van der Velde et al., 2011; Defer et al., 2015). Nevertheless, each LLS has its pros and cons. Whereas networks operating at the very-low frequencies (VLF) are able to detect lightning over large distances with relative low amount of sensors, these systems are limited in location accuracy (LA) and detection efficiency (DE) when compared to the LMA performance. On the other hand, LMAs function at very-high frequencies (VHF), thereby restricting the range of observation to very local scales and do

NHESSD
3, 5357–5381, 2015

not detect the ground stroke very well. LLS operating at low frequencies (LF) combine the best of both worlds: with baselines of a few hundred of kilometers it is possible to cover countries as well as continents (e.g. Biagi et al., 2007; Nag et al., 2011, 2013; Schulz et al., 2005; Antonescu and Burcea, 2010; Enno, 2011; Mäkelä et al., 2014), while still retaining a satisfactory level of performance in terms of LA and DE.

While most LLS provide supplementary information such as polarity and peak current of the lightning discharge, it is the spatial flash incidence that remains the main objective. This continuous interest in the spatial distribution of the lightning flash density N_g is not surprising as it is not only of importance for climatological studies, but plays a vital role in the risk analysis for protecting structures and electronic systems against damage from lightning impacts to ground (see risk management in accordance with IEC 62305-2). Various studies exist already in Europe, assessing the lightning climatology at regional scales or within country borders. For instance, Finke and Hauf (1996) observed the lightning occurrence in southern Germany and retrieved a spatial flash density of 2.8 $km^{-2} yr^{-1}$ based on a three-year data set. Schulz et al. (2005) found that over a 10-year observation period, mean flash densities vary between 0.5 and 4 flash $km^{-2} yr^{-1}$ in Austria, whereas according to Antonescu and Burcea (2010) the mean annual CG lightning density in Romania ranges from 0.34 flashes $km^{-2} yr^{-1}$ in the east to 3.06 flashes $km^{-2} yr^{-1}$ on the south, averaged over three observational years. Poelman (2014) reported CG flash densities in Belgium varying between 0.3 flashes $km^{-2} yr^{-1}$ in the west up to 2.4 $km^{-2} yr^{-1}$ toward the east of Belgium, with an average flash density of 0.7 $km^{-2} yr^{-1}$. The lowest values in Europe are found in the northern, Scandinavian countries with flash densities of about 1 $km^{-2} yr^{-1}$ in the southwest of Sweden and Baltic countries, down to 0.01 $km^{-2} yr^{-1}$ along the coast of Norway (Enno, 2011; Mäkelä et al., 2014). While it is clear that over the European continent flash densities vary from one region to another, it is not straightforward to combine latter studies into one coherent picture due to the different LLS, observational periods and grid resolutions used, as well as changes in the performance over time for a particular LLS. Another approach to investigate the European lightning density in a more coherent way is by making use of a long-range VLF lightning network. This has been done by Anderson and Klugmann (2014), presenting the observations made by the Met Office Arrival Time Difference Network (ATDnet) over Europe. However, ATDnet's observations contain, similar to other VLF networks, a certain fraction of cloud signals in addition to CG lightning (Jacobson et al., 2006; Poelman et al., 2013b), which has not been accounted for in their analysis. In addition, the spatial distribution of lightning, i.e. CG and cloud lightning, over Europe has been measured by the Optical Transient Detector (OTD) onboard the Orbview-1/Microlab satellite (Christian et al., 2003). Although OTD's measurements are useful in providing the overall spatial behavior over large areas, the absolute lightning density should be interpreted with caution as a result of the moving field of view.

In this paper we report on the cloud-to-ground lightning characteristics over most of Europe based on the observations of the European lightning location system EUCLID. Figure 1 displays the current sensor locations within the EUCLID network and the region of investigation for the following analyses. The performance of EUCLID has been frequently tested over the years in terms of its location accuracy (LA), detection efficiency (DE) and peak current estimation. For the latest in-depth analysis of the performance validation of EUCLID in Europe, the interesting reader is referred to Schulz et al. (2015). A description of the treatment of the data and methodology is provided in Sect. 2. Section 3 is reserved to display the temporal and spatial statistics along with an analysis of the multiplicity and peak current estimates. We conclude and summarize in Sect. 4.

2 Data and methodology

Since the start of EUCLID in 2001, its performance improved gradually over the years. This improvement is attributed to an increased number of sensors contributing to the network, but is also due to the upgrade of the older type of sensors into the newest LS700x sensor technology and by the implementation of advanced processing algo-

NHESSD
3, 5357–5381, 2015

rithms (Schulz et al., 2015). Nevertheless, for the purpose of this study it can be assumed that from 2006 onward the improvements to the network in terms of flash detection efficiency and location accuracy will have minor influence on the outcome presented in the remainder of this paper. This is true, since even though the stroke DE has improved, the flash DE remained rather stable since to detect a flash it is sufficient to identify successfully solely one stroke out of several in a multi-stroke flash. As such, we opt to use flash data from 2006 until 2014 in this study. In addition to CG detections, EUCLID is able to detect part of the strongest cloud-to-cloud (CC) discharges as well, using the capability of the LS700x sensors. The discrimination between CC and CG discharges is based on peak-to-zero threshold values. Note that in this work we consider each CC signal as an individual CC flash.

Initial CG stroke data has been grouped into CG flashes, with individual strokes belonging to a particular flash if $\Delta t < 1.5$ s and $\Delta r < 10$ km, with respect to the time and position of the first stroke in the flash. In addition, a temporal interstroke interval criterion, $\Delta t_{\text{interstroke}}$, of 0.5 s is used as well. These grouping criteria overlap well with those used in other studies (e.g. Cummins et al., 1998; Kuk et al., 2011), except for the more relaxed time criterion, compared to a Δt of 1 s what is traditionally used. Since occasionally flashes are observed with a duration exceeding 1 s (Poelman et al., 2013a), the time criterion used in this work is justified. The position and peak current of the first return stroke are chosen as the position and peak current of the CG flash, respectively. Note that positive discharges with peak currents smaller than 10 kA are likely to be misclassified as CG strokes when in fact those are more likely to be of intracloud nature (Cummins et al., 1998; Wacker and Orville, 1999a, b; Jerauld et al., 2005; Orville et al., 2002; Cummins et al., 2006; Biagi et al., 2007; Grant et al., 2012). Therefore, we opt to remove them from the dataset. About 5 % of all the flashes that are removed in this way are single stroke positives. In addition, after removing those particular positive strokes in a multiple-stroke flash, about 3 % of the flashes remain to be bipolar flashes. Because often positive cloud strokes are wrongly grouped to negative CG flashes, those bipolar flashes have been removed as well, such that the

NHESSD
3, 5357–5381, 2015

final flash data set contains only flashes with strokes of the same sign belonging to a particular flash.

Geographical plots are presented with a spatial resolution of $20\,\text{km}^2 \times 20\,\text{km}^2$, or stated otherwise. Note that this adopted grid size is much larger than the assumed LA of EUCLID within Europe and is therefore appropriate for this study. Moreover, it can be demonstrated that an uncertainty in flash density of less than 20 % at 90 % confidence level is obtained, when the minimum requirements are satisfied by following equation:

$$N_g \times T_{\text{obs}} \times A_{\text{cell}} \geq 80, \qquad (1)$$

with T_{obs} the observation period and A_{cell} the grid cell area expressed in years and km^2, respectively (Diendorfer, 2008). Hence, with an observation period of 9 years and a grid cell area of $400\,\text{km}^2$, regions with flash densities down to 0.02 flashes per km^2 per year are still accurately depicted in this way. Spatial distribution maps of, for example, the flash density or peak current are then obtained by summing the relevant parameter and dividing it by the amount of flashes observed per grid cell. Considering the excellent flash DE, no correction factor has been applied to the flash data in the course of this study.

3 Results and analysis

3.1 Temporal statistics

Figure 2a plots the temporal distribution of the CG stroke and flash count over the years, observed within the polygon displayed in Fig. 1. As expected, the CG activity experiences a natural annually variability, with an observed minimum of $\sim 31 \times 10^5$ flashes in 2012 and increasing up to $\sim 54 \times 10^5$ flashes in 2006. Annual variations are found as well in other parts of the globe and are attributed to the natural variability of the climate (Ghil, 2002). In addition, the CC / CG flash ratio is indicated as well. One notices a sharp increase in the CC / CG flash ratio from 2011 onward which is related to the introduction of new firmware on all the LS700x sensors in the network.

The distribution of the mean monthly flash count, including the respective ±1 SD (standard deviations), is shown in Fig. 2b. Nearly eighty-five percent of all the detected flashes occur between May and September, with a clear peak in July. On the other hand, the winter months account only for three percent of the observed lightning activity in Europe. This typical seasonal cycle is related to solar heating which peaks in European summer and favors the onset of convective storms, while on the other hand winter thunderstorms are mostly associated with the movement of cold fronts.

Figure 2c indicates the diurnal flash count as a function of local time, with a time resolution of one hour and expressed in terms of percentage of the total CG flash activity. A minimum is observed at 07:00 UTC followed by a steady increase up to the maximum point in the afternoon at 15:00 UTC. As expected, the diurnal flash count follows the diurnal temperature cycle, with about 50 % of the activity taking place between 12:00 and 18:00 UTC. The lower observed activity in the morning hours is inherent to the reduced occurrence of convective development due to solar heating of the ground and/or the atmospheric boundary layer. The overall diurnal behavior of CG flash counts in Europe overlaps well with those in other parts of the globe (Blakeslee et al., 2014).

Figure 2d displays the mean polarity distribution in Europe as a function of month. Overall, about 15 % of the observed flashes are positive, with an observed increase of positive flashes during the winter months. This pronounced increase could be related to a decrease in height of winter thunderstorms, lowering the upper positive charge of the cloud (Pinto et al., 1999), and is similar to the reports based on NLDN data (Orville and Huffines, 1999; Orville, 2001) in the US.

3.2 Flash density

Figure 3a plots the nine-year mean annual ground flash density derived from roughly 37 million CG flashes. The highest densities are found to be located over land, with most of the lightning detected at the triple point between Austria, Italy and Slovenia;

NHESSD
3, 5357–5381, 2015

The European lightning location system EUCLID – Part 2

D. R. Poelman et al.

experiencing a flash density of ~ 6 flashes km^{-2} yr^{-1} at 20 km^2 × 20 km^2 resolution. In general, densities vary in between 0.5–4 flashes km^{-2} yr^{-1} over mainland Europe, while it is clear that the Scandinavian countries and the UK experience the least amount of lightning activity in Europe. This observed spatial distribution overlaps well with the results as observed previously over Europe by the satellite-based Optical Transient Detector (OTD; Christian et al., 2003) and the ground-based long-range UK Arrival Time Difference Network (ATDnet) (Anderson and Klugmann, 2014), although the extent of densities may differ to some degree. In Fig. 3b, the geographical spread of the CC / CG flash ratio is plotted. This distribution does not resemble the true CC/CG occurrence over Europe, but is merely a measure of the capability of the LS700x sensors to detect CC signals. This is true, since the highest CC / CG ratios are found in areas where the baselines between LS700x sensors are small. For instance, Germany and some parts of France experience a high CC / CG ratio up to a factor of 4, whereas over Spain, containing only a few LS700x sensors at present, EUCLID is not efficient to detect CC signals at this moment.

Figure 4 shows the monthly flash density distribution. Note that the densities are extrapolated to whole years to attain km^{-2} yr^{-1} units. One notices that the main lightning activity over the Mediterranean and coastal sea occurs during the months September–March. This is a result of the residual heat stored in the upper water layers from previous summer, inducing convective development. Contrary to the sea, over land the majority of the activity kicks in during the summer months starting around May and ending in September, where land surface heating drives the onset of convection.

3.3 Multiplicity

The term "multiplicity" is used here to indicate the total number of strokes per flash and depends strongly on the stroke DE and adopted algorithm to group strokes into flashes. Figure 5a plots the percentage of amount of strokes detected within a single negative and positive flash. The observed percentage of single-stroke negative flashes

NHESSD
3, 5357–5381, 2015

is 55 %, and increases up to 95 % for positive flashes. 85 % of all negative flashes have been observed with three strokes or less. We find a mean multiplicity of 2.1 and 1.1 for negative and positive flashes, respectively. This is an underestimation when compared to ground truth recordings. For instance, based on ground truth recordings in Belgium, Poelman et al. (2013a) found a mean multiplicity for negative flashes of 3.7, while similar multiplicities are found in comparable ground truth studies at different regions (Rakov and Huffines, 2003; Saraiva et al., 2010; Ballarotti et al., 2012). Likewise, the high percentage of single stroke negative flashes is an overestimation with respect to ground truth observations, reporting in general values in between 20 and 40 % (Fleenor et al., 2009; Biagi et al., 2007; Poelman et al., 2013a). This overestimation of the amount of single-stroke flashes is observed by many other ground-based networks as well (Rakov and Huffines, 2003; Schulz et al., 2005; Poelman et al., 2013a) and can be related to the fact that first strokes tend to be, in general, more easily detected by a lightning location system (LLS) because of its higher peak current compared to the subsequent strokes. Additionally, outliers and misclassified cloud pulses which are not in time and distance close to another stroke influence the percentage of single-stroke flashes. As such, the amount of observed single-stroke flashes by EUCLID is increased by a fraction of multi-stroke flashes from which only one stroke is detected.

Figure 5b plots the spatial distribution of the multiplicity of negative flashes. The minimum is found at the limits of EUCLID's boundary and is a consequence of a drop in detection efficiency where only the strongest strokes within a flash tend to be detected. The spatial variance in Fig. 5b can be attributed to orography, cloud altitude and latent heat of the surface, intrinsic to specific areas. Note that a negative CG flash with a maximum multiplicity of 49 has been recorded. The latter was a flash to a tall radio and TV tower in the south of Austria, at the border of Italy and Slovenia. The overall highest multiplicities are found over the southern part of the Bay of Biscay, the Adriatic Sea and the Mediterranean Sea.

NHESSD
3, 5357–5381, 2015

3.4 Lightning peak current

Peak current estimates by EUCLID have been compared against direct measurements, made possible by dedicated instruments installed on the Gaisberg tower in Austria (Diendorfer et al., 2009). One can deduce a median peak current estimation error of 4 % compared to the measured peak currents at the Gaisberg tower (Schulz et al., 2015).

Mean/median peak current for negative and positive first strokes is −18.6/−15.0 kA and +34.5/+22.2 kA, respectively. In absolute terms, positive first strokes have higher peak currents compared to their negative counterparts. Subsequent negative strokes have mean/median peak currents of −15.2/−14.0 kA, and are hence lower compared to negative first strokes.

Figure 6a shows the cumulative statistical distribution of return stroke peak currents for negative first strokes, negative subsequent strokes, and positive strokes. It enables to view the percentage of peak currents exceeding a particular value on the horizontal logarithmic axis. The vertical axis is chosen in such a way so that a Gaussian (normal) cumulative distribution appears as a slanted straight line. The cumulative distribution for the negative first and subsequent strokes resembles almost a straight line, but is certainly not so for the positive strokes being non-linear around the low and high estimated peak currents. One deduces that about 50 % of the negative first and subsequent strokes exhibit peak currents larger than 15 kA, whereas this increases to 22 kA for positive first strokes. In general one finds that negative first strokes have higher peak currents compared to the subsequent negative strokes, but is lower than the peak currents deduced for positive strokes. The respective 95, 50 and 5 % values following the peak current distributions are summarized in Table 1.

Figure 6b plots the monthly distribution of the mean, median and 95th percentile peak current for negative and positive strokes. It is found that during the summer months the lowest values are found, with higher estimated peak currents observed toward the end/beginning of the year. Such a behavior has been demonstrated as well in the US

NHESSD
3, 5357–5381, 2015

(Brook, 1992), and is believed to be related to the observation that electric-field initiating lightning during winter is greater than during summer. Hence, discharges produced during the winter tend to exhibit more energetic discharges with higher peak currents (Brook, 1992).

Figure 7a and b display the spatial distribution of the geometric mean and 95th percentile of estimated peak current currents in negative flashes. Over large parts of mainland Europe, the mean values range in between −20 and −5 kA. However, a clear transition between land and sea alongside the Italian and Sardinian coast and the Adriatic Sea is noticed. This becomes more obvious when looking at the 95th percentile in Fig. 7b. Figure 7c zooms in on a particular interesting region in the Mediterranean Sea, indicated by the white box in Fig. 7b. This region in particular is well covered by multiple EUCLID sensors positioned inland and along the coast of France and Italy. In addition, one sensor is located in the southwest of the island Corsica. Even though the observed change in the peak current behavior is in line with the findings along the coast of US by the global GLD360 and WWLLN networks (Said et al., 2013; Hutchins et al., 2013), one can speculate that it is an artifact of the change in conductivity which is not accounted for by the central processor, or simply due to an instrumentation effect or resulting from sensor coverage issues over sea. However, apart from the findings along the US coast, Corsica is well covered by the lightning sensors and exhibits a decrease in peak current magnitude compared to the surrounding water mass. This strengthens the hypothesis that the observed peak current behavior is real. The same behavior, although less pronounced, holds for the subsequent strokes, as evidenced in Fig. 7d. In addition, the contrast between land and sea lightning becomes evident when looking at the CG flash density of negative flashes with estimated peak currents larger than 75 and 100 kA, plotted in Fig. 8a and b, respectively. It is striking that flashes with higher peak currents primarily occur in greater numbers over sea than on land.

4 Summary

Due to the variable nature of lightning occurrence from year to year, reliable insights into the lightning activity and parameters can only be achieved when based on large amounts of data. In this work, a total of 32 million CG flashes recorded in between 2006 and 2014 are used to analyze the spatial and temporal characteristics within the EUCLID domain.

It is found that the lightning activity primarily takes place between May and September, accounting for about 85 % of the total observed lightning activity. The thunderstorm season reaches its peaks in July. As regards the diurnal flash counts, those are the lowest during the morning hours, followed by a continuous increase from 10:00 UTC up to 15:00 UTC.

In addition, the observed peak current distribution displays a discrepancy between land and sea, favoring higher peak current flashes over sea than over land.

Acknowledgements. The authors are grateful to the support from all the EUCLID members.

References

Anderson, G. and Klugmann, D.: A European lightning density analysis using 5 years of ATDnet data, Nat. Hazards Earth Syst. Sci., 14, 815–829, doi:10.5194/nhess-14-815-2014, 2014.

Antonescu, B. and Burcea, S.: A cloud-to-ground lightning climatology for Romania, Mon. Weather Rev., 138, 579–591, doi:10.1175/2009MWR2975.1, 2010.

Ballarotti, M. G., Medeiros, C., Saba, M. M. F., Schulz, W., and Pinto Jr., O.: Frequency distributions of some parameters of negative downward lightning flashes based on accurate-stroke-count studies, J. Geophys. Res., 117, D06112, doi:10.1029/2011JD017135, 2012.

Biagi, C. J., Cummins, K. L. Kehoe, K. E., and Krider, E. P.: National Lightning Detection Network (NLDN) performance in southern Arizona, Texas, and Oklahoma in 2003–2004, J. Geophys. Res., 112, D05208, doi:10.1029/2006JD007341, 2007.

Blakeslee, R. J., Mach, D. M., Bateman, M. G., and Bailey, J. C.: Seasonal variations in the lightning diurnal cycle and implications for the global electric circuit, Atmos. Res., 135–136, 228–243, 2014.

Brook, M.: Breakdown of electric fields in winter storms, Res. Lett. Atmos. Elect., 12, 47–52, 1992.

Christian, H. J., Blakeslee, R. J., Boccippio, D. J., Boeck, W. L., Buechler, D. E., Driscoll, K. T., Goodman, S. J., Hall, J. M., Koshak, W. J., Mach, D. M., and Stewart, M. F.: Global frequency and distribution of lightning as observed from space by the Optical Transient Detector, J. Geophys. Res., 108, 1–15, 2003.

Cummins, K., Murphy, M., Bardo, E., Hiscox, R., Pyle, W. L., and Pifer, A.: A combined TOA/MDF technology upgrade of the U.S. National Lightning Detection Network, J. Geophys. Res., 103, 9035–9044, 1998.

Cummins, K., Cramer, J., Biagi, C., Krider, E., Jerauld, J., Uman, M., and Rakov, V.: The U.S. National Lightning Detection Network: Post-upgrade status, Second Conference on Meteorological Applications of Lightning Data, American Meteorological Society, Atlanta, Georgia, 2006.

Defer, E., Pinty, J.-P., Coquillat, S., Martin, J.-M., Prieur, S., Soula, S., Richard, E., Rison, W., Krehbiel, P., Thomas, R., Rodeheffer, D., Vergeiner, C., Malaterre, F., Pedeboy, S., Schulz, W., Farges, T., Gallin, L.-J., Ortéga, P., Ribaud, J.-F., Anderson, G., Betz, H.-D., Meneux, B., Kotroni, V., Lagouvardos, K., Roos, S., Ducrocq, V., Roussot, O., Labatut, L., and Molinié, G.: An overview of the lightning and atmospheric electricity observations collected in southern France during the HYdrological cycle in Mediterranean EXperiment (HyMeX), Special Observation Period 1, Atmos. Meas. Tech., 8, 649–669, doi:10.5194/amt-8-649-2015, 2015.

Diendorfer, G.: Some comments on the achievable accuracy of local ground flash density values, Proc. 29th Int. Conf. on Lightning Protection, Uppsala, Sweden, 6 pp., 2008.

Diendorfer, G., Pichler, H., and Mair, M.: Some parameters of negative upward-initiated lightning to the Gaisberg tower (2000–2007), IEEE Trans. Electromagn. Compat., 51, 443–452, 2009.

Enno, S. E.: A climatology of cloud-to-ground lightning over Estonia, 2005–2009, Atmos. Res., 100, 310–317, 2011.

Finke, U. and Hauf, T.: The characteristics of lightning occurrence in southern Germany, Beitr. Phys. Atmos., 69, 361–374, 1996.

NHESSD

3, 5357–5381, 2015

The European lightning location system EUCLID – Part 2

D. R. Poelman et al.

Fleenor, S. A., Biagi, C. J., Cummins, K. L., Krider, E. P., and Shao, X.-M.: Characteristics of cloud-to-ground lightning in warm-season thunderstorms in the central Great Plains, Atmos. Res., 91, 333–352, doi:10.1016/J.atmosres.2008.08.011, 2009.

Ghil, M.: Natural climate variability. Encyclopedia of global environmental change, in: Volume 1: The Earth System: physical and chemical dimensions of global environmental change, edited by: MacCracken, M. C. and Perry, J. S., John Wiley & Sons, Ltd, Chichester, 2002.

Grant, M. D., Nixon, K. J., and Jandrell, I. R.: Positive polarity: misclassification between intracloud and cloud-to-ground discharges in the Southern African Lightning Detection Network, Proceedings, 22nd International Lightning Detection Conference, Broomfield, Colorado, USA, 2012.

Hutchins, M. L., Holzworth, R. H., Virts, K. S., Wallace, J. M., and Heckman, S.: Radiated VLF energy differences of land and oceanic lightning, Geophys. Res. Lett., 40, 2390–2394, doi:10.1002/grl.50406, 2013.

Jacobson, A. R., Holzworth, R., Harlin, J., Dowden, R., and Lay, E.: Performance assessment of the World Wide Lightning Location Network (WWLLN), using the Los Alamos Sferic Array (LASA) as ground truth, J. Atmos. Ocean. Tech., 23, 1082–1092, 2006.

Jerauld, J., Rakov, V. A., Uman, M. A., Rambo, K. J., Jordan, D. M., Cummins, K. L., and Cramer, J. A.: An evaluation of the performance characteristics of the U.S. National Lightning Detection Network in Florida using rocket-triggered lightning, J. Geophys. Res., 110, D19106, doi:10.1029/2005JD005924, 2005.

Keogh, S. J., Hibbett, E., Nash, J., and Eyre, J.: The Met Office Arrival Time Difference (ATD) system for thunderstorms detection and lightning location, Forecasting Research Tech. Rep. 488, Met Office, Numerical Weather Prediction UK, 22 pp., 2006.

Krehbiel, P. R., Thomas, R. J., Rison, W., Hamlin, T., Harlin, J., and Davis, M.: Three dimensional lightning mapping observations during MEaPRS in central Oklahoma, Proc. 11th Conf. Atmos. Electr., Guntersville, AL, 376–379, 1999.

Kuk, B. J., Kim, H. I., Ha, J. S., and Lee, H. K.: Intercomparison study of cloud-to-ground lightning flashes observed by KARITLDS and KLDN at South Korea, J. Appl. Meteorol. Clim., 50, 224–232, 2011.

Mäkelä, A., Enno, S. E., and Haapalainen, J.: Nordic lightning information system: thunderstorm climate of northern Europe for the period 2002–2011, Atmos. Res., 139, 46–61, 2014.

Nag, A., Mallick, S., Rakov, V. A., Howard, J., Biagi, C. J., Hill, D., Uman, M. A., Jordan, D. M., Rambo, K. J., Jerauld, J., DeCarlo, B. A., Cummins, K. L., and Cramer, J. A.:

Evaluation of U.S. National Lightning Detection Network performance characteristics using rocket-triggered lightning data acquired in 2004–2009, J. Geophys. Res., 116, D02123, doi:10.1029/2010JD014929, 2011.

Nag, A., Murphy, M. J., Cummins, K. L., Pifer, A. E., and Cramer, J. A.: Upgrade of the U.S. National Lightning Detection Network in 2013, Preprints Intl. Symp. Lightning Protection (XII SIPDA), Belo Horizonte, Brazil, 5 pp., 2013.

Orville, R. E.: Cloud-to-ground lightning in the United States: NLDN results in the first decade, 1989–98, Mon. Weather Rev., 129, 1179–1193, 2001.

Orville, R. E. and Huffines, G. R.: Lightning ground flash measurements over the contiguous United States: 1995–97, Mon. Weather Rev., 127, 2693–2703, 1999.

Orville, R. E., Huffines, G., Burrows, W., Holle, R., and Cummins, K.: The North American Lightning Detection Network (NLDN) – First results: 1998–2000, Mon. Weather Rev., 130, 2098–2108, 2002.

Rakov, V. A. and Huffines, G. R.: Return-Stroke Multiplicity of Negative Cloud-to-Ground Lightning Flashes, J. Appl. Meteorol., 42, 1455–1462, 2003.

Rison, W., Krehbiel, P., Thomas, R., Hamlin, T., and Harlin, J.: A time-of-arrival lightning mapping system with high time resolution, presented at the Fall Meeting Amer. Geophys. Union, San Francisco, CA, 2000.

Rison, W. R., Scott, R., Thomas, R. J., Krehbiel, P. R., Hamlin, T., and Harlin, J.: 3-dimensional lightning and dual-polarization observations of thunderstorms in central New Mexico, Proc. 11th Int. Conf. Atmos. Electr., Guntersville, AL, 432–435, 1999.

Pinto, O., Jr., Pinto, I. R. C. A., Gomes, M. A. S. S., Vitorello, I., Padilha, A. L., Diniz, J. H., Carvalho, A. M., and Filho, A. C.: Cloud-to-ground lightning in southeastern Brazil in 1993: 1. Geographical distribution, J. Geophys. Res., 104, 31369–31379, doi:10.1029/1999JD900800, 1999.

Poelman, D. R.: A 10-year study on the characteristics of thunderstorms in Belgium based on cloud-to-ground lightning data, Mon. Weather Rev., 142, 4839–4849, 2014.

Poelman, D. R., Schulz, W., and Vergeiner, C.: Performance characteristics of distinct lightning detection networks covering Belgium, J. Atmos. Ocean. Tech., 30, 942–951, doi:10.1175/JTECH-D-12-00162.1, 2013a.

Poelman, D. R., Honoré, F., Anderson, G., and Pedeboy, S.: Comparing a regional, subcontinental, and long-range lightning location system over the Benelux and France, J. Atmos. Ocean. Tech., 30, 2394–2405, doi:10.1175/JTECH-D-12-00263.1, 2013b.

NHESSD
3, 5357–5381, 2015

Said, R. K., Inan, U. S., and Cummins, K. L.: Long-range lightning geolocation using a VLF radio atmospheric waveform bank, J. Geophys. Res., 115, D23108, doi:10.1029/2010JD013863, 2010.

Said, R. K., Murphy, M. J., Demetriades, N. W. S., Cummins, K. L., and Inan, U. S.: Methodology and performance estimates of the GLD360 lightning detection network, Proc. 14th Int. Conf. on Atmospheric Electricity, ICAE, Rio de Janeiro, Brazil, 4 pp., 2011.

Said, R. K., Cohen, M. B., and Inan, U. S.: Highly intense lightning over the oceans: Estimated peak currents from global GLD360 observations, J. Geophys. Res.-Atmos., 118, 6905-6915, doi:10.1002/jgrd.50508, 2013.

Saraiva, A. C. V., Saba, M. M. F., Pinto Jr., O., Cummins, K. L., Krider, E. P., and Campos, L. Z. S.: A comparative study of negative cloud-to-ground lightning characteristics in São Paulo (Brazil) and Arizona (United States) based on high-speed video observations, J. Geophys. Res., 115, D11102, doi:10.1029/2009JD012604, 2010.

Schulz, W., Cummins, K., Diendorfer, G., and Dorninger, M.: Cloud-to-ground lightning in Austria: A 10-year study using data from a lightning location system, J. Geophys. Res., 110, D09101, doi:10.1029/2004JD005332, 2005.

Schulz, W., Diendorfer, G., Pedeboy, S., and Poelman, D. R.: The European lightning location system EUCLID – Part 1: Performance validation, Nat. Hazards Earth Syst. Sci. Discuss., 15, 5325–5355, doi:10.5194/nhessd-15-5325-2015, 2015.

van der Velde, O., Montanya, J., Rison, B., Aulich, G., Pineda, N., Soula, S., Romero, D., Rico, R., and Reglero, V.: First Results of the Lightning Mapping Array in the Ebro Delta, American Geophysical Union Fall Meeting, 5–9 December 2011, San Francisco, USA, 2011.

Wacker, R. and Orville, R.: Changes in measured lightning flash count and return stroke peak current after the 1994 U.S. National Lightning Detection Network Upgrade: 1. Observations, J. Geophys. Res., 104, 2151–2157, 1999a.

Wacker, R. and Orville, R.: Changes in measured lightning flash count and return stroke peak current after the 1994 U.S. National Lightning Detection Network Upgrade: 2. Theory, J. Geophys. Res., 104, 2159–2162, 1999b.

Table 1. Peak current cumulative statistical distribution values.

	Percentage exceeding tabulated value		
Peak current [kA]	95 %	50 %	5 %
First neg. strokes	4	15	57
Subseq. neg. strokes	5	14	35
First pos. strokes	10	22	96

NHESSD
3, 5357–5381, 2015

The European lightning location system EUCLID – Part 2

D. R. Poelman et al.

Figure 1. Sensor locations within the EUCLID network. Note that only data within the polygon (dash-dotted line) is used for quantitative analysis in this work.

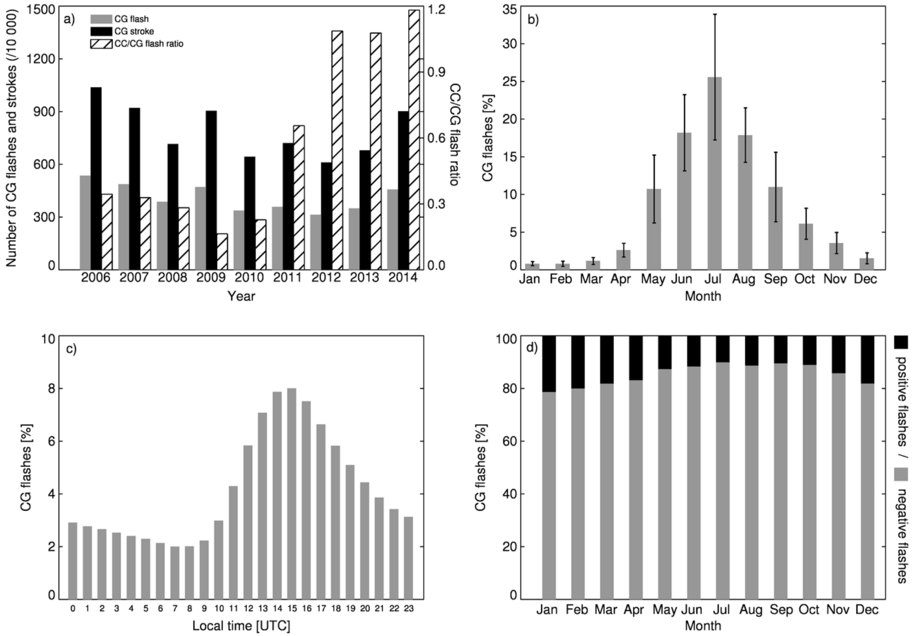

Figure 2. (a) Variation of the annual CG stroke and flash counts, as well as the CC / CG flash ratio, **(b)** mean monthly flash counts with bars representing the ±1 SD (standard deviation), **(c)** mean diurnal flash counts and **(d)** mean monthly polarity distribution, based on 2006–2014 EUCLID data.

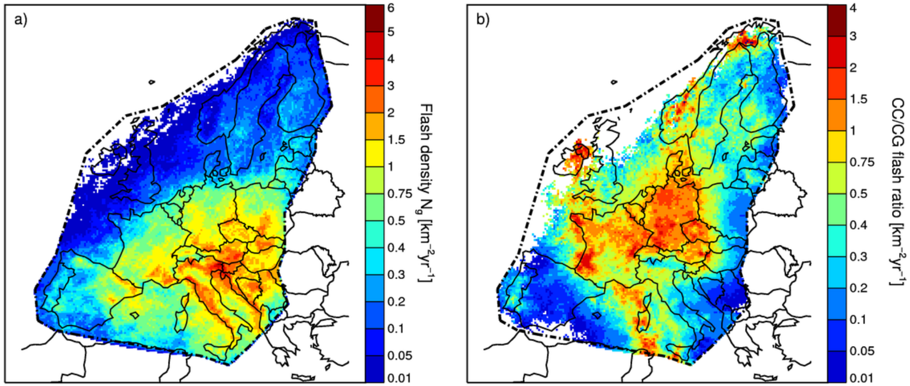

Figure 3. **(a)** Mean annual CG flash density [$km^{-2}\,yr^{-1}$], and **(b)** CC / CG flash density ratio [$km^{-2}\,r^{-1}$], based on 2006–2014 EUCLID data and adopting a spatial resolution of $20\,km^2 \times 20\,km^2$.

NHESSD

3, 5357–5381, 2015

The European lightning location system EUCLID – Part 2

D. R. Poelman et al.

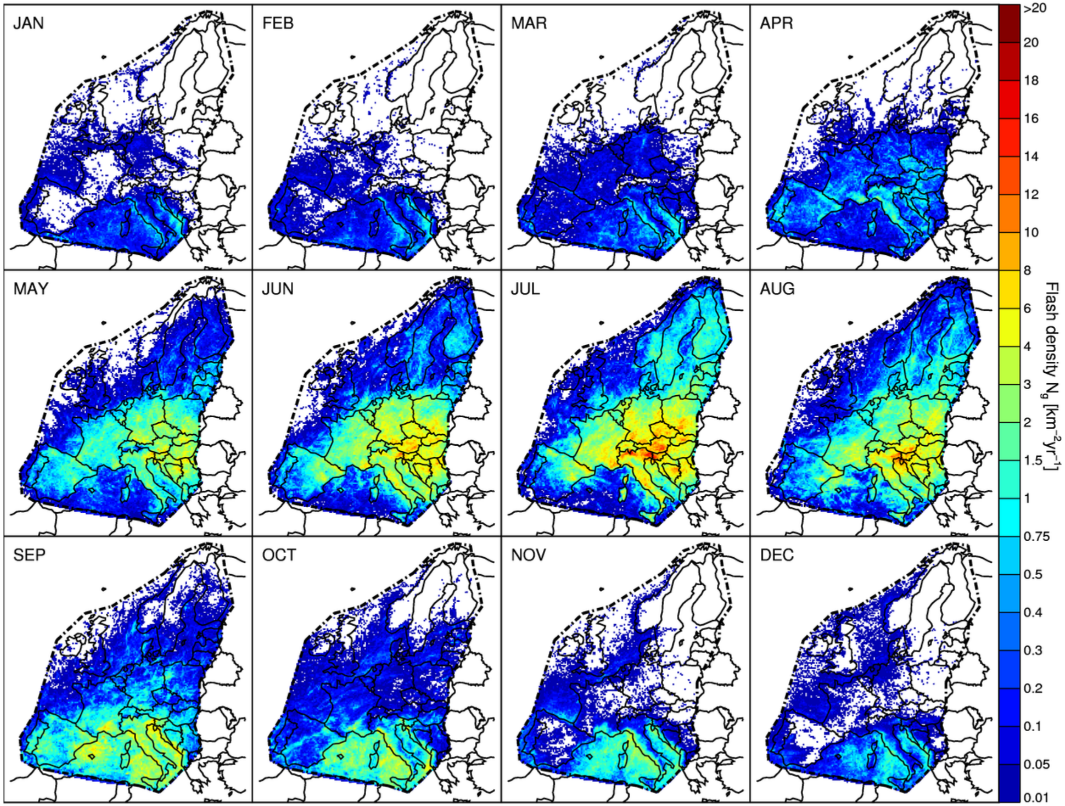

Figure 4. Monthly variability of flash density N_g [km^{-2} yr^{-1}], based on 2006–2014 EUCLID data and adopting a spatial resolution of 20 km^2 × 20 km^2.

NHESSD
3, 5357–5381, 2015

The European lightning location system EUCLID – Part 2

D. R. Poelman et al.

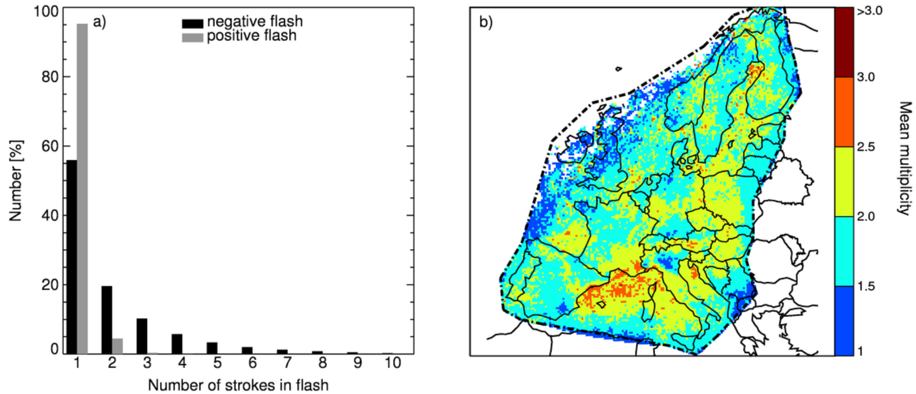

Figure 5. (a) Histogram of the percentage of strokes per flash for negative (black) and positive (grey) flashes, and **(b)** multiplicity distribution of negative flashes, based on 2006–2014 EUCLID data and adopting a spatial resolution of 20 km^2 × 20 km^2.

NHESSD
3, 5357–5381, 2015

The European lightning location system EUCLID – Part 2

D. R. Poelman et al.

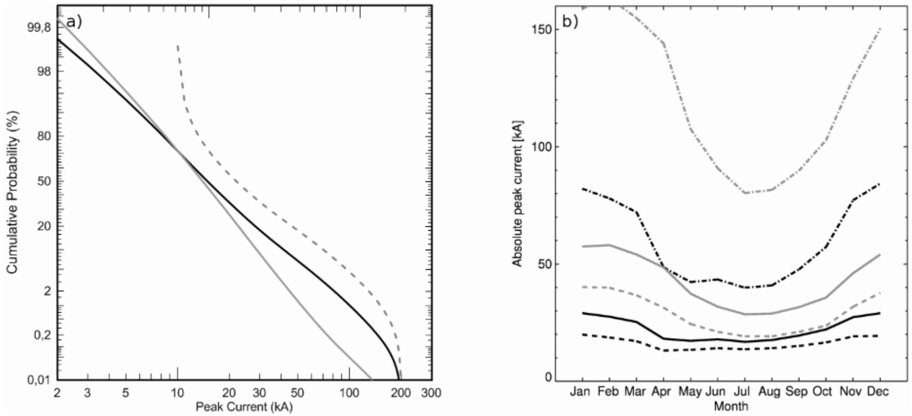

Figure 6. (a) Cumulative statistical distribution of return-stroke peak currents for negative first strokes (black solid), negative subsequent (grey solid), and positive first strokes (grey dashed). **(b)** Peak current distribution as a function of month for negative (black) mean (solid), median (dashed), 95th percentile (dash-dotted) and for positive (grey) mean (solid), median (dashed), 95th percentile (dash-dotted) strokes.

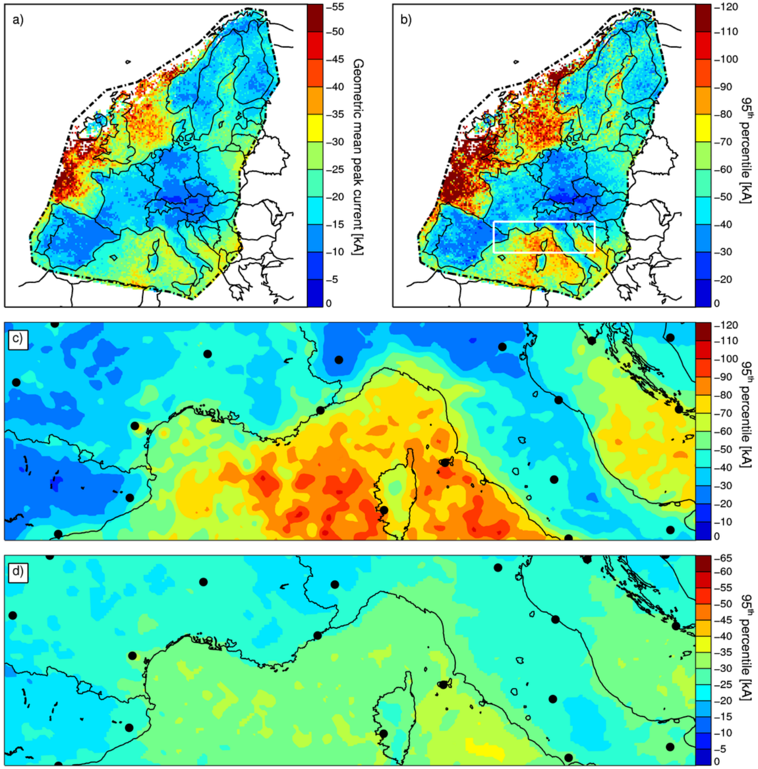

Figure 7. Distribution of **(a)** geometric mean, and **(b)** 95th percentile of the peak current [kA] from first strokes in negative flashes, based on 2006–2014 EUCLID data and adopting a spatial resolution of 20 $km^2 \times 20$ km^2. **(c)** Zoom-in as outlined by the white box in **(b)**, smoothed by a Gaussian filter for clarity. **(d)** Same as **(c)**, but for subsequent strokes. In addition, the sensor locations are indicated in **(c)** and **(d)**.

NHESSD
3, 5357–5381, 2015

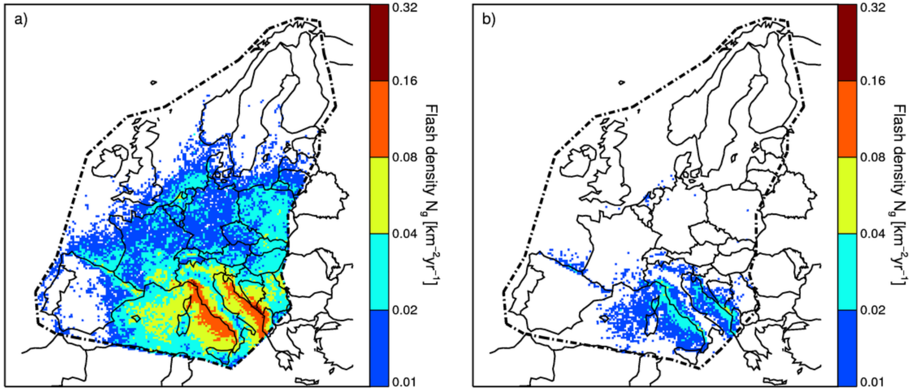

Figure 8. Mean annual flash density [$km^{-2}\,yr^{-1}$] of CG flashes with estimated absolute peak current above **(a)** 75 kA and **(b)** 125 kA.

NHESSD
3, 5357–5381, 2015